Successful Prediction of Positron Emission Tomography–Imaged Metformin Hepatic Uptake Clearance in Humans Using the Quantitative Proteomics–Informed Relative Expression Factor Approach

ⓘMadhav Sachar, Vineet Kumar, Lars C. Gormsen, Ole Lajord Munk, and
ⓘJashvant D. Unadkat

Department of Pharmaceutics, University of Washington, Seattle, Washington (M.S., V.K., J.D.U.) and Department of Nuclear Medicine and PET Center, Aarhus University Hospital, Aarhus N, Denmark (L.C.G., O.L.M.)

ABSTRACT

Predicting transporter-mediated in vivo hepatic drug clearance (CL) from in vitro data (IVIVE) is important in drug development to estimate first-in-human dose and the impact of drug interactions and pharmacogenetics on hepatic drug CL. For IVIVE, one can use human hepatocytes and the traditional milligrams of protein content per gram of liver tissue (MGPGL) approach. However, this approach has been found to consistently underpredict the observed in vivo hepatic drug CL. Therefore, we hypothesized that using transporter-expressing cells and the relative expression factor (REF), determined using targeted quantitative proteomics, will accurately predict in vivo hepatic CL of drugs. We have successfully tested this hypothesis in rats with rosuvastatin, which is transported by hepatic Organic anion transporting polypeptides (OATPs). Here, we tested this hypothesis for another drug and another transporter; namely, organic cation transporter (OCT)1-mediated hepatic distributional CL of metformin. First, we estimated the in vivo metformin hepatic sinusoidal uptake CL ($CL_{h,s,in}$) of metformin by reanalysis of previously published human positron emission tomography imaging data. Next, using the REF approach, we predicted the in vivo metformin $CL_{h,s,in}$ using OCT1-transporter–expressing HEK293 cells or plated human hepatocytes. Finally, we compared this REF-based prediction with that using the MGPGL approach. The REF approach accurately predicted the in vivo metformin hepatic $CL_{h,s,in}$, whereas the MGPGL approach considerably underpredicted the in vivo metformin $CL_{h,s,in}$. Based on these and previously published data, the REF approach appears to be superior to the MGPGL approach for a diverse set of drugs transported by different transporters.

SIGNIFICANCE STATEMENT

This study is the first to use organic cation transporter 1-expressing cells and plated hepatocytes to compare proteomics-informed REF approach with the traditional MGPGL approach to predict hepatic uptake CL of metformin in humans. The proteomics-informed REF approach, which corrected for plasma membrane abundance, accurately predicted the positron emission tomography–imaged metformin hepatic uptake CL, whereas the MGPGL approach consistently underpredicted this CL.

Introduction

Predicting transporter-mediated in vivo clearance of drugs from in vitro data (IVIVE) is important in drug development to estimate first-in-human dose and interindividual variability in drug clearance (CL) due to drug interactions and pharmacogenetics. For IVIVE of hepatic metabolic CL of a drug, the relative activity factor (RAF) (with or without a probe drug) is traditionally used. When used without a probe drug, this approach scales the in vitro intrinsic metabolic CL of the drug to that in vivo using hepatocellularity or milligrams of protein microsomal protein yield per gram of liver tissue (Obach et al., 1997;

Andersson et al., 2001). When used with a probe drug, the probe drug must selectively measure the intrinsic CL (CL_{int}) of drug by a single enzyme. An alternative approach, the relative expression factor (Rostami-Hodjegan and Tucker, 2007; Soars et al., 2007; Rowland et al., 2011), is used where in vitro metabolic CL_{int} of the drug (e.g., in recombinant enzymes) is scaled to that in vivo using the ratio of the abundance of the enzyme in vivo (e.g., hepatic tissue) to that in vitro (e.g., in recombinant enzymes).

Although using RAF for IVIVE of metabolic CL has been successful (Rostami-Hodjegan and Tucker, 2007; Soars et al., 2007; Rowland et al., 2011), predicting transport-mediated CL using this approach results in underestimation of the observed in vivo CL of the drug (Jones et al., 2012). In addition, the magnitude of this misprediction is not uniform across drugs (Jones et al., 2012). Therefore, generalization across drugs cannot be made through the use of a "common" empirical scaling factor.

ABBREVIATIONS: CL, clearance; $CL_{h,s,in}$, hepatic sinusoidal uptake clearance; CL_{int}, intrinsic clearance; $CL_{int,in\ vitro}$, intrinsic in vitro uptake clearance; HK HEPES-buffered, Krebs-Ringer bicarbonate; OATP, organic anion transporting polypeptides; OCT, organic cation transporter; IVIVE, in vitro to in vivo extrapolation; MGPGL, milligrams of protein content per gram of liver tissue; PET, positron emission tomography; PHH, plated human hepatocyte; PMA, plasma membrane abundance; REF, relative expression factor; THTR2, thiamine transporter 2; WSHM, well stirred model.

Moreover, because the RAF requires selective probe substrate and primary human cells (e.g., hepatocytes), this approach cannot be used where selective transporter probe substrates are not available (e.g., OATP substrates) or when primary cells from the organ of interest are not available or validated (e.g., blood-brain endothelial cells/kidney epithelial cells). Therefore, we have hypothesized that the REF approach, coupled with quantitative targeted proteomics, can overcome many of these problems and be used for accurate IVIVE of transporter-mediated CL of drugs. However, like any other approach, the accuracy of REF-based predictions needs to be verified. Indeed, we along with others have shown that this approach can be used to successfully predict in vivo transporter-mediated CL (Bosgra et al., 2014; Vildhede et al., 2016; Ishida et al., 2018; Kumar et al., 2018) and hepatic concentrations of rosuvastatin (an OATP substrate) obtained through positron emission tomography (PET) imaging (Bosgra et al., 2014; Vildhede et al., 2016; Ishida et al., 2018; Kumar et al., 2018). However, this success needs to be tested with other drugs transported by other transporters, such as metformin, which is transported into the liver by OCT1 and possibly by OCT3 and THTR2 (Liang et al., 2015; Pakkir Maideen et al., 2017). Therefore, we first estimated the in vivo hepatic sinusoidal uptake CL ($CL_{h,s,in}$) of [^{11}C]metformin by reanalysis of previously published PET imaging data (Gormsen et al., 2016). This reanalysis was conducted to correct for hepatic blood [^{11}C]metformin content not conducted in that publication. Next, using the REF approach, we predicted the in vivo metformin $CL_{h,s,in}$ using transporter-expressing cells and plated human hepatocytes (PHH). These predictions were compared with that obtained using the milligrams of protein content per gram of liver tissue (MGPGL) approach (i.e., RAF without probe drug). Our prediction of the in vivo metformin $CL_{h,s,in}$ was considered a success if it fell within 2-fold of the observed value.

Materials and Methods

Chemicals and Reagents. Specific synthetic peptides and corresponding stable labeled peptides for OCT1, Na$^+$/K$^+$ ATPase, and calreticulin were purchased form New England Peptides (Boston, MA). Bicinchoninic acid assay kit, dithiothreitol, iodoacetamide, mass spectrometry–grade trypsin, pierce cell-surface protein isolation kit, High-performance liquid chromatography-grade acetonitrile, Dulbecco's phosphate-buffered saline, and Dulbecco's modified Eagle's medium high-glucose medium were purchased form Thermo Fisher Scientific (Rockford, IL). Metformin (hydrochloride salt), thiamine (hydrochloride salt), quinidine, potassium chloride, magnesium sulfate, D-glucose, HEPES, sodium chloride, sodium bicarbonate, calcium chloride dipotassium phosphate, and formic acid were purchased from Sigma-Aldrich (St. Louis, MO). [^{14}C]Metformin hydrochloride (114 mCi/mmol) was obtained from Moravek Biochemicals, Inc. (Brea, CA). Collagen-coated 24-well plates were purchased from Corning (Kennebunk, ME). Human hepatocyte thaw medium, INVITROGRO HI medium, INVITROGRO CP medium, and TORPEDO antibiotic mix, as well as cryopreserved human hepatocytes (PHH), were generously provided by BioIVT (Westbury, NY). OCT1-HEK293 cells were generously provided by SOLVO Biotechnology (Hungary).

Determination of Metformin Uptake CL_{int} into OCT1-HEK293 Cells and Human Hepatocytes (PHH). OCT1-HEK293 cells were grown in T-75 cm^2 flasks with 20 ml of high-glucose Dulbecco's modified Eagle's medium supplemented with 10% fetal bovine serum, 2 mM L-glutamine, 100 IU/ml penicillin, and 100 mg/ml streptomycin. Medium was changed daily, and cells were kept in a humidified incubator with 5% carbon dioxide at 37°C. For uptake assays, 0.5 million HEK293 cells per well were plated in a 24-well plate for 24 hours. For uptake assays using PHH, cryopreserved hepatocytes were thawed and plated 0.35 million per well in a 24-well collagen-coated plate with 0.5 ml/well TORPEDO containing INVITROGRO CP medium (1:9 v/v) for 5 hours.

To determine [^{14}C]metformin uptake, HEK293 cells or PHH were washed three times with HEPES-buffered Krebs-Ringer bicarbonate buffer (HK buffer)

(4.8 mM KCl, 1.2 mM K$_2$HPO$_4$, 1.2 mM MgSO$_4$, 5.6 mM glucose, 25 mM HEPES, 12 mM CaCl$_2$, 125 mM NaCl, 25 mM NaHCO$_3$) and incubated at 37°C. To initiate uptake, 500 μl of HK buffer containing 5 or 20 μM [^{14}C]metformin (for HEK293 cells or PHH, respectively) with or without inhibitor (preincubated at 37°C) was added to the cells. After an appropriate time (over a period in which uptake was linear; 5 minutes for HEK293 cells and 15 minutes for PHH), [^{14}C]metformin uptake into the cells was terminated by removing [^{14}C]metformin-containing solution and immediately washing it three times with ice-cold HK buffer. Then, cells were lysed by adding 1 ml of 2% SDS solution to each well and incubating them on a shaker at 125 rpm for 1 hour at 37°C. After 1 hour, 700 μl of lysed solution from each well was used to measure radioactivity by Tri-Carb Liquid Scintillation Counters (PerkinElmer, Waltham, MA). In addition, 50 μl of lysed solution was used to measure protein content using the bicinchoninic acid assay method. [^{14}C]Metformin uptake CL into the cells was calculated by the ratio of rate of [^{14}C]metformin uptake and the [^{14}C]metformin concentration in the media. Uptake $CL_{int,in\ vitro}$ was calculated by dividing the slope of [^{14}C]metformin accumulation over time by [^{14}C]metformin concentration in media. CL_{int} calculated in absence and presence of inhibitor was considered as total CL ($CL_{int,total}$) and passive CL ($CL_{int,in\ vitro,passive}$), respectively. Active CL ($CL_{int,in\ vitro,active}$) was calculated by subtracting $CL_{int,in\ vitro,passive}$ from $CL_{int,in\ vitro,total}$.

To determine the contribution of OCT1 or thiamine transporter 2 (THTR2) to [^{14}C]metformin transport into PHH, [^{14}C]metformin uptake assays were conducted in the presence or absence of 500 μM quinidine or 400 mM thiamine [a THTR2 substrate with Km of 3.4 mM (Liang et al., 2015)], respectively.

Quantification of Total and Percent Plasma Membrane Abundance of OCT1 in HEK293 Cells. Data for the total and PMA of OCT1 in PHH were obtained from our previous publication (Kumar et al., 2019). OCT1 total and PMA in HEK293 cells was quantified using our previously published biotinylation approach (Kumar et al., 2017). HEK293 cells were grown in three independent experiments in a 75-cm^2 flask until 80% confluency and incubated at 37°C with 10 ml of 0.78 mg/ml sulfo-NHS-SS-biotin. After 1 hour, cells were lysed, and 50 μl of cell lysate was separated to quantify total abundance. From the rest of the total cell lysate, the biotinylated plasma membrane fragments (to quantify %PMA) were separated from the total cell lysate and intracellular membranes using the neutravidin resin columns. Briefly, 0.2 mg of total protein homogenate and biotinylated fraction were denatured by adding 45 μl of 100 mM ammonium bicarbonate buffer (pH 7.8), 25 μl of 3% sodium deoxycholate (w/v), 12.5 μl of 250 mM dithiothreitol, and 5 μl of 10 mg/ml human albumin and incubated at 95°C for 5 minutes. After incubation, samples were returned to room temperature, 25 μl of 200 mM iodoacetamide was added, and samples were incubated in the dark for 30 minutes. Then, 500 μl of ice-cold methanol, 200 μl of chloroform, and
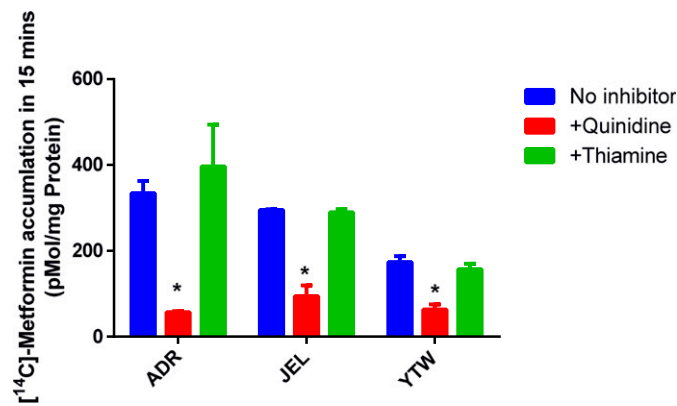

Fig. 1. [^{14}C]Metformin uptake into three lots of PHH in the absence and presence of an OCT1 or a THTR2 inhibitor. Quinidine (500 μM), an OCT inhibitor, significantly inhibited hepatocyte uptake of metformin, whereas thiamine (400 mM), a THTR2 inhibitor, did not. Data are presented as means ± S.D. of triplicate determinations. Data were analyzed by one-way analysis of variance followed by Tukey multiple comparison post hoc test. *$P < 0.05$ compared with the respective control.
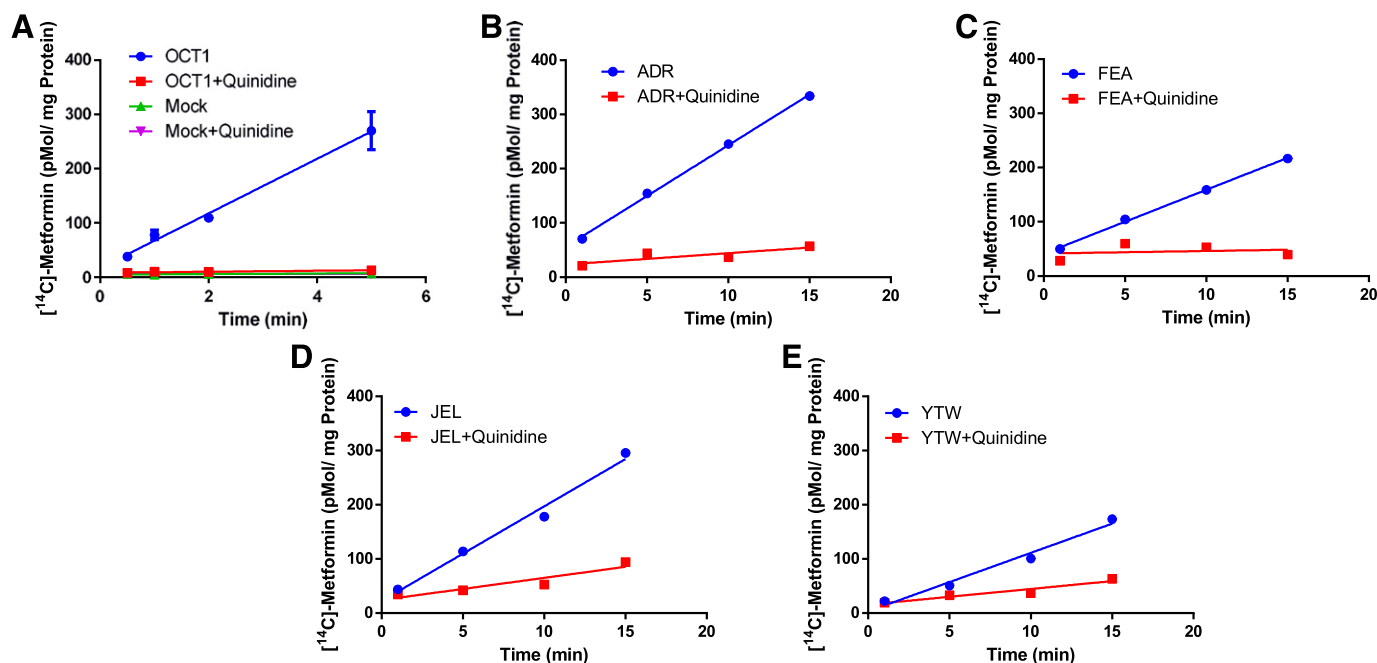
Fig. 2. Estimation of [^{14}C]metformin uptake CL$_{int}$ into HEK 293 cells or PHH. [^{14}C]Metformin uptake into OCT1-expressing HEK293 and mock cells (A) or into four different lots of PHH (B–E) was linear over a period of 5 and 15 minutes, respectively. Data in (A–E) are presented as means ± S.D. of experiments conducted in triplicate.

450 μl of water were added. Samples were mixed and centrifuged at 12,000g for 10 minutes. Precipitated protein samples were redissolved in 45 μl of 100 mM ammonium bicarbonate buffer and digested with 20 μl (~3.2 μg) of trypsin for 18 hours at 37°C in a shaker (300 rpm). Finally, the digestion was terminated by adding to the sample 20 μl of ice-cold acetonitrile containing the internal standard. Then, the sample was centrifuged at 5000g for 5 minutes at 4°C. The supernatant was collected and analyzed on AB Sciex 6500 triple-quadrupole mass spectrometer (Sciex, Framingham, MA) coupled to the Water Acquity Ultra-Performance Liquid Chromatography (UPLC) system (Waters Corporation, Milford, MA) operated in electrospray positive ionization mode using a previously described approach (Prasad et al., 2016). An Acquity UPLC HSS T3 Column (1.8 mm, 2.1 100 mm) with 0.2-mm inlet frits (Waters) was used for chromatographic separation and resolution. The flow rate of the mobile phase was 0.3 ml/min using a gradient ranging from 3% to 90% acetonitrile/water containing 0.1% formic acid. Signature peptides and product ions as well as their respective Stable Isotope Labelled (SIL) peptides used to quantify proteins were obtained from our previous report (Kumar et al.,

2019). The ratio of abundance of protein in biotinylated fractions and total lysate was used to determine %PMA.

Estimation of In Vivo [^{11}C]Metformin CL$_{h,s,in}$ by Compartmental Modeling of PET Imaging Data. PET-imaged metformin hepatic radioactivity concentration-time data previously published by Gormsen et al. (2016) were reanalyzed using a blood input function and a one-tissue compartment model (Fig. 3A) with a fixed blood volume (SAAMII). This differed from the published analysis, in which radioactivity from the volume of blood within the liver tissue was not taken into account, plasma concentrations were used as input, and a two-compartment model was used (Gormsen et al., 2016).

$$\frac{dA_L}{dt} = CL_{h,s,in} \cdot C_B - CL_{h,s,ef} \cdot C_L \qquad (1)$$

$$C_B = C_{Venous} \cdot 0.8 + C_{Arterial} \cdot 0.2, \qquad (2)$$

where A, C, B, L, CL$_{h, s, in}$, and CL$_{h,s,ef}$ represent amount, concentration, blood, liver, sinusoidal uptake CL, sinusoidal efflux CL, biliary efflux CL, and metabolic CL respectively. Since no biliary efflux was observed and the majority of metformin is excreted renally unchanged, biliary clearance and metabolic clearance were not
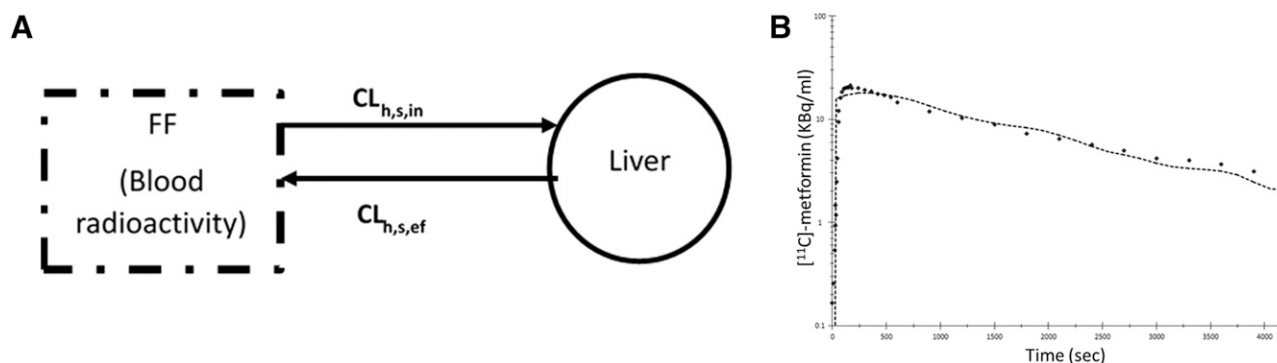

Fig. 3. Estimate of the in vivo [^{11}C]metformin hepatic uptake clearance after correcting for blood [^{11}C]metformin content in the liver. [^{11}C]Metformin hepatic concentrations calculated from PET imaging and corresponding plasma [^{11}C]metformin concentrations were obtained from a previous publication (Gormsen et al., 2016). A one-compartment pharmacokinetic model (A), which incorporated correction for blood [^{11}C]metformin content in the liver, was fitted to the hepatic [^{11}C]metformin concentration vs. time data in five subjects. Arterial plus image–estimated portal venous blood [^{11}C]metformin concentrations were used as the input function using the forcing function (FF) approach. Observed (diamonds) and model-fitted hepatic [^{11}C]metformin concentration vs. time profile in a representative subject demonstrates relatively good fit of the model to the data (B).Where CL$_{h,s,in}$ is hepatic sinusoidal uptake clearance and CL$_{h,s,ef}$ is hepatic sinusoidaleflux clearance

TABLE 1

Total and passive [14C]metformin (500 μM) uptake clearances (CL$_{int,in\ vitro}$) into PHH and HEK293 cells estimated in the absence and presence of quinidine, respectively

Cell	CL$_{int,in\ vitro}$ (μl/min per milligram protein)[a]	
	−Quinidine	+Quinidine
HEK293: OCT1	8.27 ± 5.8	0.22 ± 0.06
HEK293: Mock	0.17 ± 0.10	0.29 ± 0.007
PHH: ADR	0.88	0.07
PHH: FEA	0.64	0.04
PHH: JEL	0.79	0.15
PHH: YTW	0.55	0.10

[a]From either three (HEK293 cells; mean ± S.D.) or two independent experiments (PHH; mean).

TABLE 2

Estimate of [11C]metformin hepatic uptake clearance from the PET imaging study

Subject	CL$_{h,s,in}$ (ml/min)		
	Value	%CV[a]	95% CI[a]
1	388	34	127–650
2	361	26	155–568
3	552	30	226–878
4	427	38	102–751
5	476	25	236–715
Mean ± S.D.	441 ± 76		

CI, confidence interval.
[a]%CV and 95% CI represent the confidence in the CL$_{h,s,in}$ (milliliters per minute) estimate.

included in eq. 1 (Hardie, 2007; Graham et al., 2011; Gormsen et al., 2016). The hepatic input blood concentration is a sum of the input via the portal vein (80%) and the hepatic artery (20%) (Schenk et al., 1962), where C$_{Arterial}$ and C$_{Venous}$ are the observed [11C]metformin arterial and portal vein concentrations, respectively (eq. 2). The volume of the liver was determined based on eq. 3 (Chan et al., 2006).

$$\text{Liver weight (g)} = 218.32 + \text{body weight (kg)} \times 12.29 + \text{gender} \times 50.74 \tag{3}$$

For male and female, sex = 1 and 0, respectively. The volume of blood in the liver was fixed to 10% of total blood volume, estimated based on body weight (75 ml/kg for males and 65 ml/kg for females) (Lautt, 1977; Stabin and Siegel, 2003; Pham and Shaz, 2013). Goodness of fit of the model to the data was assessed by the weighted residual plots, visual inspection of the predicted and observed data, and the confidence (CV%) in the estimates of the parameters.

Prediction of the In Vivo Metformin Blood Hepatic Uptake CL from PHH Using the MGPGL Approach. Metformin in vivo blood intrinsic hepatic sinusoidal uptake CL (CL$_{int,s,in}$) was predicted from PHH data using the MGPGL approach (eq. 4).

$$CL_{int,s,in} = \frac{CL_{int,PHH,total} \times \text{Liver weight} \times \text{MGPGL}}{B:P} \tag{4}$$

Liver weight was assumed to be 1500 g, B:P is the blood-to-plasma ratio (0.6), and MGPGL was 120 mg of total protein per gram of liver based on a previous report (1.2×10^8 cells per gram of liver and 1 million cells ~1 mg protein) (Jones et al., 2012; Gormsen et al., 2016; Kim et al., 2019).

Then, metformin sinusoidal uptake clearance was computed using the well stirred model (WSHM).

$$CL_{h,s,in} = \frac{Q*fu* \ CL_{int,s,in}}{Q + fu* \ CL_{int,s,in}}, \tag{5}$$

where fu is the fraction of metformin unbound in plasma (assumed to be 1), and Q is the hepatic blood flow (1500 ml/min) (Scheen, 1996).

Prediction of In Vivo Metformin Hepatic Uptake CL from OCT1-HEK293 Cells and PHH Using the REF Approach. In vivo blood metformin hepatic intrinsic sinusoidal active uptake CL (CL$_{int,s,active\ in}$) was determined from in vitro metformin uptake CL in OCT1-HEK293 cells or PHH using the REF approach, corrected for OCT1 PMA in these cells or PHH (%PMA$_{in\ vitro}$; eq. 6). In doing so, the following assumptions were made: 1) OCT1 is the only transporter responsible for metformin hepatic uptake (see *Results* for justification) and 2) because it is impossible to use the biotinylation method for quantification of OCT1 PMA in liver tissue, the PMA abundance of OCT1 in liver tissue (%PMA$_{ex\ vivo}$) was assumed to be 100%.

$$CL_{int,s,active\ in} = \frac{CL_{int,in\ vitro,active} \times \frac{[E]_{ex\ vivo}}{[E]_{in\ vitro}} \times \frac{\%PMA_{ex\ vivo}}{\%PMA_{in\ vitro}} \times \text{MGMPGL} \times \text{Liver weight}}{B:P} \tag{6}$$

[E]$_{in\ vitro}$ is OCT1 abundance in HEK293 cells or PHH. [E]$_{ex\ vivo}$ is total OCT1 abundance in human liver tissue, and MGMPGL is milligrams of total membrane

protein per gram of liver from individual control liver ($n = 36$) obtained from our previous report (Wang et al., 2016).

Also, the blood hepatic intrinsic sinusoidal passive uptake CL of metformin (CL$_{int,s,passive\ in}$) was scaled based on liver weight and adjusted for the sinusoidal surface area (SSA) (37%; eq. 7) since the entire plasma membrane of hepatocytes is not exposed to blood (Esteller, 2008). The correction for SSA was not made for the active uptake of metformin into cells since OCT1 is thought to be present only on the sinusoidal membrane of the hepatocytes.

$$CL_{int,s,passive,in} = \frac{CL_{int,in\ vitro,passive} \times \text{MGPGL} \times \% \ SSA \times \text{Liver weight}}{B:P} \tag{7}$$

Finally, the total blood intrinsic hepatic sinusoidal uptake CL (CL$_{int,s,in}$) was computed (eq. 8) to estimate the sinusoidal hepatic uptake clearance (CL$_{h,s,in}$) using the WSHM (eq. 5).

$$CL_{int,s,in} = CL_{h,s,active\ in} + CL_{h,s,passive\ in} \tag{8}$$

Data are presented as means of REF-predicted CL$_{h,s,in}$ based on 36 control livers, whereas the mean MGPGL-predicted CL$_{h,s,in}$ was computed as a mean of four different lots of PHH.

Results

[14C]Metformin Uptake into Hepatocytes Is Mediated by OCT1 and Not THTR2. Since [14C]metformin uptake was linear in PHH over a period of 15 minutes (Fig. 2), this was the time used to determine [14C] metformin uptake into PHH in the presence and absence of OCT (quinidine) or THTR2 (thiamine) inhibitor (Fig. 1). Quinidine, but not thiamine, significantly inhibited metformin uptake by 83%, 68.1%, and 63.5% in ADR, JEL, and YTW PHH, respectively.

Estimation of [14C]Metformin CL$_{int}$ Uptake into HEK293 Cells or PHH. [14C]Metformin uptake into HEK293 cells and PHH was linear over 5 and 15 minutes, respectively (Fig. 2). The mean [14C] metformin CL$_{int,PHH,passive}$ or CL$_{int,OCT1-HEK293,passive}$ was similar to CL$_{int,mock-HEK293,total}$ or CL$_{int,mock-HEK293,passive}$. These data further confirm that [14C]metformin uptake into hepatocytes is mediated primarily by OCT1 (Table 1).

Plasma and Total Membrane Abundance of OCT1 in OCT1-HEK293 Cells and PHH. The percent PMAs of OCT1, Na$^+$/K$^+$ ATPase (plasma membrane marker), and calreticulin (endoplasmic reticulum marker) in HEK293 cells were 36.04% ± 2.46%, 58.73% ± 2.79%, and 6.63% ± 0.39%, respectively. The low presence of calreticulin in the plasma membrane fraction demonstrated the fidelity of the biotinylation method. The percent PMA of OCT1 in PHH used in this study (ADR: 63.8%, FEA: 55.3%, JEL: 51.9%, YTW: 65.8%) was obtained from our previous report (Kumar et al., 2019). These PMA data, together with the total abundance of OCT1 in these cells, were used (eq. 5) to predict the in vivo metformin hepatic uptake clearance (see below and Table 4).
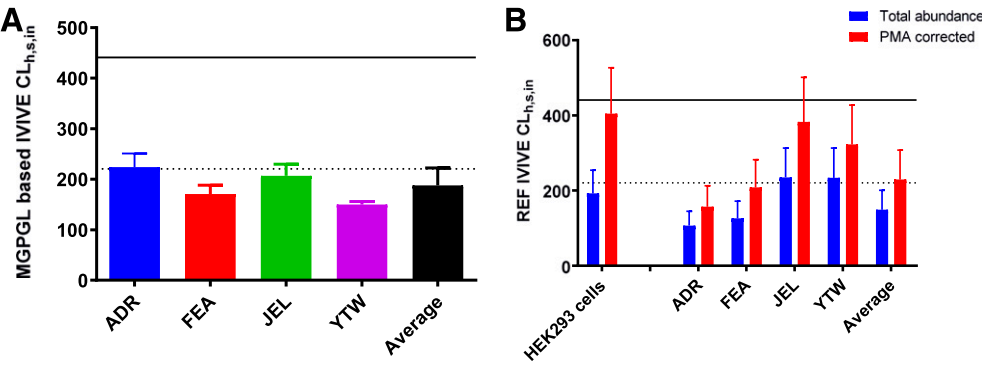
Fig. 4. In vitro to in vivo extrapolation of metformin $CL_{h,s,in}$ based on HEK293 cells or PHH. For all four lots of PHH, the predicted $CL_{h,s,in}$ based on the MGPGL approach underpredicted the observed value (continuous line) and also fell outside the 2-fold predefined acceptance criteria (dashed line, A). Likewise, the predicted metformin $CL_{h,s,in}$ based on total abundance of OCT1 (i.e., without correcting for PMA) in HEK293 cells or PHH underpredicted the observed value (B). In contrast, after correcting for PMA, the predicted metformin $CL_{h,s,in}$ based on HEK293 cells or the average PHH was within the predefined acceptance criteria, with the latter underpredicting the observed value more than the former. Data shown are means ± S.D.

Estimating In Vivo [^{11}C]Metformin Hepatic Uptake CL from PET Imaging Data after Correcting for Blood [^{11}C]Metformin Content in the Liver. The mean estimate of [^{11}C]metformin $CL_{h,s,in}$ in four subjects was 441 ± 76 ml/min (range 361–552 ml/min), with each subject's $CL_{h,s,in}$ estimated with a high degree of confidence (low %CV of the estimates) (Table 2).

IVIVE of Metformin Hepatic Sinusoidal Uptake CL from HEK293 Cells and PHH Using REF Versus the MGPGL Approach. IVIVE of metformin $CL_{h,s,in}$ based on the MGPGL approach significantly underpredicted (by more than 56%) the observed value (Fig. 4A; Table 3). Likewise, IVIVE of metformin $CL_{h,s,in}$ based on total abundance of OCT1 (i.e., without correcting for PMA) in HEK293 cells or PHH underpredicted the observed value (Fig. 4B; Table 4). In addition, except for PHH JEL and YTW, the predicted $CL_{h,s,in}$ based on HEK293 cells or PHH (average or ADR or FEA) was below the predefined acceptance criteria for prediction of the observed in vivo $CL_{h,s,in}$. In contrast, after correcting for PMA, the predicted $CL_{h,s,in}$ based on HEK293 cells or the average PHH was within predefined acceptance criteria, with the latter underpredicting the observed value much more than the former.

Discussion

The major findings of this study are as follows: 1) metformin is transported into human hepatocytes predominantly by OCT1 with no (or little) contribution from THTR2; 2) PET imaging data should be corrected for hepatic blood metformin content to correctly estimate the in vivo metformin $CL_{h,s,in}$; and 3) the REF approach is superior to the MGPGL approach in accurately predicting the in vivo $CL_{h,s,in}$ of metformin.

In humans, hepatic uptake of metformin (the site of its pharmacological effect) is purely a distributional CL because metformin is not metabolized or excreted into the bile by the liver and is primarily (99%) eliminated unchanged in the urine (Pentikainen et al., 1979). The latter

was confirmed in the human PET imaging study, in which no metformin radioactivity could be detected in the gallbladder (Gormsen et al., 2016). Various in vitro studies have confirmed that metformin is transported into the liver primarily by OCT1 (Km 1.2 mM) (Kimura et al., 2005). Although OCT3 can transport metformin (Km 1.1 mM) (Chen et al., 2010), because the hepatic protein abundance of OCT3, relative to OCT1, is negligible (Drozdzik et al., 2019), we assumed that it did not contribute to the total uptake of metformin either in vivo or in vitro. THTR2, a thiamine transporter, has also been found to transport metformin (Km 1.15 mM) (Liang et al., 2015). Therefore, we determined its contribution in the transport of metformin into PHH using a sufficiently high concentration (400 mM) of thiamine to completely inhibit THTR2. We found that THTR2 does not significantly contribute to metformin transport into PHH (Fig. 1). This was confirmed by our findings that metformin uptake CL into PHH was similar to that in OCT1-HEK293 cells when OCT1 was completely inhibited by quinidine in both systems (Fig. 2; Table 1).

Prior to predicting metformin $CL_{h,s,in}$ by scaling $CL_{int, in vitro}$ in OCT1-HEK293 cells or PHH, we estimated the in vivo metformin $CL_{h,s,in}$ by reanalysis of previously published PET imaging data. Reanalysis was performed because estimates of hepatic uptake CL (whether in vivo or in vitro into hepatocytes) of a drug are primarily derived from data in the initial uptake phase. In the case of PET imaging, because the liver has a significant amount of blood (10% of total blood volume) and the radioactivity content in hepatic tissue during the initial uptake phase may not be significantly larger than that in the blood, the drug content in the blood in the liver will upwardly bias the true hepatic uptake CL of the drug. Indeed, this was the case for metformin: the previously reported [^{11}C]metformin plasma $CL_{h,s,in}$ was 0.55 ± 0.15 ml/min per milliliter (or 0.55 ± 0.15 ml/min per gram; assuming density of liver tissue as 1.0) of hepatic tissue (or blood $CL_{h,s,in}$ 1375 ± 375 ml/min assuming 1.5 kg as liver weight by PET imaging) (Gormsen et al., 2016). On reanalysis of these PET imaging data, in which we took into

TABLE 3

IVIVE of metformin $CL_{h,s,in}$ based on the traditional MGPGL approach

	PHH				
	ADR	FEA	JEL	YTW	Average ± S.D.
$CL_{int,PHH,total}$ (μl/min per milligram protein)	0.88 ± 0.12	0.64 ± 0.07	0.79 ± 0.10	0.55 ± 0.02	0.72 ± 0.15
Protein yield MGPGL (mg protein/g of liver)			120[a]		
Assumed liver weight (g)			1500		
Predicted $CL_{h,s,in}$ (ml/min) (eq. 4)	264 ± 37	193 ± 22	240 ± 32	167 ± 7	216 ± 44
$CL_{h,s,in}$ (ml/min) based on the WSHM (eq. 5)	225 ± 28	171 ± 17	206 ± 24	150 ± 5	188 ± 34

[a]Value for the yield of total milligrams of protein per gram of liver was obtained based on hypocellularity and total protein per million hepatocytes (Jones et al., 2012; Kim et al., 2019).

TABLE 4
IVIVE of metformin $CL_{h,s,in}$ based on the REF approach

	HEK293	PHH				
		ADR	FEA	JEL	YTW	Average ± S.D.
$CL_{int,\,in\,vitro,active}$ (μl/min per milligram protein)	8.05 ± 0.64	0.81 ± 0.06	0.60 ± 0.05	0.65 ± 0.45	0.45 ± 0.08	0.63 ± 0.15
$CL_{int,\,in\,vitro,passive}$ (μl/min per milligram protein)	0.22 ± 0.06	0.07 ± 0.06	0.04 ± 0.02	0.15 ± 0.07	0.1 ± 0.06	0.09 ± 0.05
In vitro total OCT1 protein abundance (pmol/mg protein)	17.34 ± 0.35	3.21 ± 0.12[a]	1.92 ± 0.33[a]	1.04 ± 0.06[a]	0.71 ± 0.04[a]	1.72 ± 1.12
Ex vivo hepatic tissue OCT1 protein abundance (pmol/mg protein)[b]		4.68 ± 1.9				3.75 ± 2.28
Scaling factor: $[E]_{ex\,vivo}/[E]_{in\,vitro}$	0.27	1.46	2.43	4.5	6.59	
Protein yield MGMPGL (mg total membrane protein/g of liver)[b]		37.68				
Protein yield MGPGL (mg total protein/g of liver)[c]		120				
IVIVE $CL_{h,s,in}$ assuming 100% plasma membrane abundance (ml/min) (eqs. 6–8)	224 ± 81	116 ± 44	139 ± 55	285 ± 109	284 ± 111	168 ± 64
IVIVE $CL_{h,s,in}$ based on the WSHM and assuming 100% plasma membrane abundance (ml/min) (eq. 5)	192 ± 62	107 ± 38	126 ± 46	235 ± 78	234 ± 79	149 ± 52
%PMA	36 ± 2.5	64 ± 9.3[a]	55 ± 6.4[a]	52 ± 11.5[a]	66 ± 4.2[a]	59 ± 6.7
IVIVE $CL_{h,s,in}$ corrected for OCT1 PMA (eq. 6)	578 ± 225	178 ± 69	248 ± 99	535 ± 210	425 ± 169	277 ± 109
IVIVE $CL_{h,s,in}$ based on the WSHM and corrected for OCT1 PMA (eq. 5)	405 ± 122	157 ± 56	208 ± 74	382 ± 119	323 ± 105	230 ± 78

[a] OCT1 abundance and %PMA were obtained from our previous report (Kumar et al., 2019).
[b] Each hepatic tissue (n = 36) OCT1 total abundance and the corresponding protein yield MGMPGL were obtained from our previous report (Wang et al., 2016).
[c] Value for the yield of total milligrams of protein per gram of liver was obtained based on hypocellularity and total protein per million hepatocytes (Jones et al., 2012; Kim et al., 2019).

consideration the significant presence of blood in the liver, the estimated $CL_{h,s,in}$ was found to be 441 ml/min, i.e., ~32% of the previously reported values (Table 2).

When we used the REF approach to predict $CL_{h,s,in}$ based on the assumption that 100% of OCT1 was present on the plasma membrane of both HEK293 cells or PHH (average abundance), the $CL_{h,s,in}$ was underpredicted by ~60% for both in vitro systems (Fig. 4; Table 4). The predicted $CL_{h,s,in}$ by the individual lots of hepatocytes was also underpredicted, but that by the JEL and YTW was within 2-fold of the acceptance criteria. Since only OCT1 present in the plasma membrane is functional, and not all the OCT1 transporters are present in the plasma membrane of HEK293 cells or PHH, we asked whether correcting for PMA of OCT1 improved our prediction of $CL_{h,s,in}$. This question was also motivated by our previous finding that such a correction allowed for better prediction of in vivo metformin secretory renal CL in humans (Kumar et al., 2018). Indeed, after correcting for PMA, OCT1-HEK293 cells predicted a value for $CL_{h,s,in}$ (405 ± 122 ml/min) that was not significantly different from that observed from PET imaging (441 ± 76 ml/min). Likewise, after correcting for PMA, data from the PHH, on average, predicted a value for $CL_{h,s,in}$ (230 ± 78 ml/min) that was within the lower limit of 2-fold predefined acceptance criteria (221 ml/min). In addition, except for ADR and FEA, the remaining lots of PHH predicted metformin $CL_{h,s,in}$ within the predefined acceptance criteria. In contrast, the traditional MGPGL approach (on average) underpredicted $CL_{uptake,h}$ by more than 56% (ranging from 47% to 64%) (Fig. 4A; Table 3). This observation is consistent with previous reports that PHH underpredicts the hepatic uptake CL of several drugs (Jones et al., 2012). One possible reason proposed for such underprediction is the protein-mediated effect on hepatic uptake CL (Miyauchi et al., 2018; Bteich et al., 2019). However, this is unlikely to explain our findings since metformin is not bound to plasma proteins. Another potential explanation is that the value of MGPGL used is incorrect. Taken together these results clearly demonstrate that the PMA-corrected REF approach is superior to the traditional MGPGL approach when predicting $CL_{h,s,in}$ of metformin. We have also demonstrated that the REF approach is superior to the MGPGL approach when predicting $CL_{h,s,in}$ of rosuvastatin (an OATP substrate) in rat (Ishida et al., 2018). Thus, the REF approach appears to be superior to the MGPGL approach for a diverse set of drugs that are transported by different transporters. Additional studies need to be conducted to determine whether this conclusion can be generalized across a larger number of drugs transported by a variety of transporters.

Acknowledgments

Authorship Contributions

Participated in research design: Sachar, Kumar, Unadkat.
Conducted experiments: Sachar.
Performed data analysis: Sachar.
Wrote or contributed to the writing of the manuscript: Sachar, Munk, Gormsen, Unadkat.

References

Andersson TB, Sjöberg H, Hoffmann KJ, Boobis AR, Watts P, Edwards RJ, Lake BG, Price RJ, Renwick AB, Gómez-Lechón MJ, et al. (2001) An assessment of human liver-derived in vitro systems to predict the in vivo metabolism and clearance of almokalant. *Drug Metab Dispos* **29**: 712–720.
Bosgra S, van de Steeg E, Vlaming ML, Verhoeckx KC, Huisman MT, Verwei M, and Wortelboer HM (2014) Predicting carrier-mediated hepatic disposition of rosuvastatin in man by scaling from individual transfected cell-lines in vitro using absolute transporter protein quantification and PBPK modeling. *Eur J Pharm Sci* **65**:156–166.

Bteich M, Poulin P, and Haddad S (2019) The potential protein-mediated hepatic uptake: discussion on the molecular interactions between albumin and the hepatocyte cell surface and their implications for the in vitro-to-in vivo extrapolations of hepatic clearance of drugs. *Expert Opin Drug Metab Toxicol* **15**:633–658.

Chan SC, Liu CL, Lo CM, Lam BK, Lee EW, Wong Y, and Fan ST (2006) Estimating liver weight of adults by body weight and gender. *World J Gastroenterol* **12**:2217–2222.

Chen L, Pawlikowski B, Schlessinger A, More SS, Stryke D, Johns SJ, Portman MA, Chen E, Ferrin TE, Sali A, et al. (2010) Role of organic cation transporter 3 (SLC22A3) and its missense variants in the pharmacologic action of metformin. *Pharmacogenet Genomics* **20**:687–699.

Drozdzik M, Busch D, Lapczuk J, Muller J, Ostrowski M, Kurzawski M, and Oswald S (2019) Protein abundance of clinically relevant drug transporters in the human liver and intestine: a comparative analysis in paired tissue specimens. *Clin Pharmacol Ther* **105**:1204–1212.

Esteller A (2008) Physiology of bile secretion. *World J Gastroenterol* **14**:5641–5649.

Gormsen LC, Sundelin EI, Jensen JB, Vendelbo MH, Jakobsen S, Munk OL, Hougaard Christensen MM, Brøsen K, Frøkiær J, and Jessen N (2016) In vivo imaging of human 11C-metformin in peripheral organs: dosimetry, biodistribution, and kinetic analyses. *J Nucl Med* **57**:1920–1926.

Graham GG, Punt J, Arora M, Day RO, Doogue MP, Duong JK, Furlong TJ, Greenfield JR, Greenup LC, Kirkpatrick CM, et al. (2011) Clinical pharmacokinetics of metformin. *Clin Pharmacokinet* **50**:81–98.

Hardie DG (2007) AMP-activated protein kinase as a drug target. *Annu Rev Pharmacol Toxicol* **47**:185–210.

Ishida K, Ullah M, Tóth B, Juhasz V, and Unadkat JD (2018) Successful prediction of in vivo hepatobiliary clearances and hepatic concentrations of rosuvastatin using sandwich-cultured rat hepatocytes, transporter-expressing cell lines, and quantitative proteomics. *Drug Metab Dispos* **46**:66–74.

Jones HM, Barton HA, Lai Y, Bi YA, Kimoto E, Kempshall S, Tate SC, El-Kattan A, Houston JB, Galetin A, et al. (2012) Mechanistic pharmacokinetic modeling for the prediction of transporter-mediated disposition in humans from sandwich culture human hepatocyte data. *Drug Metab Dispos* **40**:1007–1017.

Kim SJ, Lee KR, Miyauchi S, and Sugiyama Y (2019) Extrapolation of in vivo hepatic clearance from in vitro uptake clearance by suspended human hepatocytes for anionic drugs with high binding to human albumin: improvement of in vitro-to-in vivo extrapolation by considering the "albumin-mediated" hepatic uptake mechanism on the basis of the "facilitated-dissociation model". *Drug Metab Dispos* **47**:94–103.

Kimura N, Masuda S, Tanihara Y, Ueo H, Okuda M, Katsura T, and Inui K (2005) Metformin is a superior substrate for renal organic cation transporter OCT2 rather than hepatic OCT1. *Drug Metab Pharmacokinet* **20**:379–386.

Kumar V, Nguyen TB, Tóth B, Juhasz V, and Unadkat JD (2017) Optimization and application of a biotinylation method for quantification of plasma membrane expression of transporters in cells. *AAPS J* **19**:1377–1386.

Kumar V, Salphati L, Hop C, Xiao G, Lai Y, Mathias A, Chu X, Humphreys WG, Liao M, Heyward S, et al. (2019) A comparison of total and plasma membrane abundance of transporters in suspended, plated, sandwich-cultured human hepatocytes versus human liver tissue using quantitative targeted proteomics and cell surface biotinylation. *Drug Metab Dispos* **47**:350–357.

Kumar V, Yin J, Billington S, Prasad B, Brown CDA, Wang J, and Unadkat JD (2018) The importance of incorporating OCT2 plasma membrane expression and membrane potential in IVIVE of metformin renal secretory clearance. *Drug Metab Dispos* **46**:1441–1445.

Lautt WW (1977) Hepatic vasculature: a conceptual review. *Gastroenterology* **73**:1163–1169.

Liang X, Chien HC, Yee SW, Giacomini MM, Chen EC, Piao M, Hao J, Twelves J, Lepist EI, Ray AS, et al. (2015) Metformin is a substrate and inhibitor of the human thiamine transporter, THTR-2 (SLC19A3). *Mol Pharm* **12**:4301–4310.

Miyauchi S, Masuda M, Kim SJ, Tanaka Y, Lee KR, Iwakado S, Nemoto M, Sasaki S, Shimono K, Tanaka Y, et al. (2018) The phenomenon of albumin-mediated hepatic uptake of organic anion transport polypeptide substrates: prediction of the in vivo uptake clearance from the in vitro uptake by isolated hepatocytes using a facilitated-dissociation model. *Drug Metab Dispos* **46**:259–267.

Obach RS, Baxter JG, Liston TE, Silber BM, Jones BC, MacIntyre F, Rance DJ, and Wastall P (1997) The prediction of human pharmacokinetic parameters from preclinical and in vitro metabolism data. *J Pharmacol Exp Ther* **283**:46–58.

Pakkir Maideen NM, Jumale A, and Balasubramaniam R (2017) Drug interactions of metformin involving drug transporter proteins. *Adv Pharm Bull* **7**:501–505.

Pentikäinen PJ, Neuvonen PJ, and Penttilä A (1979) Pharmacokinetics of metformin after intravenous and oral administration to man. *Eur J Clin Pharmacol* **16**:195–202.

Pham HP and Shaz BH (2013) Update on massive transfusion. *Br J Anaesth* **111** (Suppl 1):i71–i82.

Prasad B, Johnson K, Billington S, Lee C, Chung GW, Brown CD, Kelly EJ, Himmelfarb J, and Unadkat JD (2016) Abundance of drug transporters in the human kidney cortex as quantified by quantitative targeted proteomics. *Drug Metab Dispos* **44**:1920–1924.

Rostami-Hodjegan A and Tucker GT (2007) Simulation and prediction of in vivo drug metabolism in human populations from in vitro data. *Nat Rev Drug Discov* **6**:140–148.

Rowland M, Peck C, and Tucker G (2011) Physiologically-based pharmacokinetics in drug development and regulatory science. *Annu Rev Pharmacol Toxicol* **51**:45–73.

Scheen AJ (1996) Clinical pharmacokinetics of metformin. *Clin Pharmacokinet* **30**:359–371.

Schenk WG Jr., McDonald JC, McDonald K, and Drapanas T (1962) Direct measurement of hepatic blood flow in surgical patients: with related observations on hepatic flow dynamics in experimental animals. *Ann Surg* **156**:463–471.

Soars MG, McGinnity DF, Grime K, and Riley RJ (2007) The pivotal role of hepatocytes in drug discovery. *Chem Biol Interact* **168**:2–15.

Stabin MG and Siegel JA (2003) Physical models and dose factors for use in internal dose assessment. *Health Phys* **85**:294–310.

Vildhede A, Mateus A, Khan EK, Lai Y, Karlgren M, Artursson P, and Kjellsson MC (2016) Mechanistic modeling of pitavastatin disposition in sandwich-cultured human hepatocytes: a proteomics-informed bottom-up approach. *Drug Metab Dispos* **44**:505–516.

Wang L, Collins C, Kelly EJ, Chu X, Ray AS, Salphati L, Xiao G, Lee C, Lai Y, Liao M, et al. (2016) Transporter expression in liver tissue from subjects with alcoholic or hepatitis C cirrhosis quantified by targeted quantitative proteomics. *Drug Metab Dispos* **44**:1752–1758.

Address correspondence to: Dr. Jashvant D. Unadkat, Department of Pharmaceutics, Box 357610, University of Washington, Seattle, WA 98195. E-mail: jash@uw.edu